Biomolecules and Biomedicine
ISSN: 2831-0896 (Print) | ISSN: 2831-090X (Online)
Journal Impact Factor® (2024): 2.2
CiteScore® (2024): 5.2
www.biomolbiomed.com | blog.bjbms.org

RESEARCH ARTICLE

Toprak et al: del Nido vs St. Thomas II cardioplegia

Comparing del Nido and St. Thomas II cardioplegia in a rat ischemia–reperfusion model: Histopathology, mitochondria, and TEM analysis

Burak Toprak[1*], Abdulkadir Bilgiç[2], Murat Özeren[2], Ebru Ballı[3]

[1]Department of Cardiovascular Surgery, Mersin City Education and Research Hospital, Mersin, Türkiye;

[2]Department of Cardiovascular Surgery, Mersin University Faculty of Medicine Hospital, Mersin, Türkiye;

[3]Department of Histology, Mersin University Faculty of Medicine Hospital, Mersin, Türkiye.

*Correspondence to Burak Toprak: brk.tprk@gmail.com.

DOI: https://doi.org/10.17305/bb.2025.13394

ABSTRACT

Myocardial ischemia–reperfusion (IR) injury remains a major challenge in cardiac surgery, and comparative histological and ultrastructural data on cardioplegia solutions are limited. This study compared the myocardial protective effects of St. Thomas II and del Nido cardioplegia in a controlled rat IR model, focusing on inflammation, mast cell dynamics, and subcellular preservation. Twenty-four Wistar Albino rats were randomized to Control, St. Thomas II, or del Nido groups. After 90 minutes of ischemia and 30 minutes of passive reperfusion, myocardial tissue was analyzed by hematoxylin–eosin, toluidine blue, and transmission electron microscopy. Outcomes included mast cell counts, leukocyte infiltration, karyolysis, and ultrastructural measures (Flameng score, crista density, basement membrane thickness). Both cardioplegia groups preserved myocardial morphology and attenuated inflammatory changes versus control. Light microscopy revealed a consistent mast cell density and reduced karyolysis in hearts treated with cardioplegia, with no significant differences observed between St. Thomas II and del Nido solutions. Conversely, transmission electron microscopy (TEM), the primary endpoint of this study, demonstrated enhanced mitochondrial and endothelial preservation in the del Nido group, as evidenced by significantly lower Flameng scores and increased crista density compared to both St. Thomas II and control groups ($p < 0.05$). In conclusion, both solutions reduced early IR-related injury, but del Nido provided a significant ultrastructural advantage on TEM despite similar routine light-microscopic findings.

Keywords: Cardioplegia, myocardial ischemia, reperfusion injury, del Nido, St. Thomas II, transmission electron microscopy, histopathology, rat model.

INTRODUCTION

Myocardial protection is a critical concern in cardiac surgery due to the ischemic period that follows aortic cross-clamping and cardiopulmonary bypass [1,2]. Ischemia-reperfusion (IR) injury significantly contributes to postoperative morbidity and mortality [3], and various strategies—including hypothermia and cardioplegia—have been developed to mitigate this damage [4,5].

Cardioplegia solutions suppress myocardial metabolism and reduce reperfusion injury by inducing diastolic arrest. However, optimal composition and delivery methods remain under debate [6]. Among these, St. Thomas II is a classical crystalloid solution commonly used in adults, offering reliable arrest but requiring repeated dosing [7,8]. In contrast, del Nido cardioplegia, initially designed for pediatric cases, has gained acceptance in adults for its single-dose efficacy, sodium-channel blockade via lidocaine, and antioxidant effect via mannitol [9,10]. St. Thomas II is a classical depolarizing crystalloid cardioplegia composed of high potassium and magnesium concentrations, producing diastolic arrest through membrane depolarization and requiring repeated dosing during prolonged ischemia. In contrast, del Nido cardioplegia is a polarized, low-calcium, lidocaine-containing solution that provides extended single-dose arrest with additional myocardial protection through sodium-channel blockade and mannitol-mediated free-radical scavenging. These compositional and mechanistic differences form the conceptual basis of our comparison [7–10], and are consistent with previous histological investigations comparing crystalloid cardioplegic formulations [8,11]. While some studies suggest comparable clinical outcomes between the two solutions in terms of mortality and arrhythmia [11], few have examined their differential histological effects.

Mast cells, recognized for their role in early myocardial inflammation, contribute to IR injury through release of histamine, cytokines, and proteases [12,13]. Yet, their histological dynamics in cardioplegia-protected myocardium remain poorly characterized. Given their early activation and their potential to amplify endothelial dysfunction, leukocyte infiltration, and tissue remodeling, mast cells represent a pivotal but underexplored target for evaluating cardioprotective efficacy. In addition to conventional histological assessment, transmission electron microscopy (TEM) provides a unique advantage in identifying ultrastructural alterations that precede visible light-microscopic injury. Mitochondrial swelling, cristae disruption, and

sarcomeric disorganization are well-established early markers of ischemia–reperfusion damage [14]. However, only a limited number of experimental studies have compared the ultrastructural impact of cardioplegic solutions using TEM, with recent investigations by Jung et al. providing early evidence for solution-dependent mitochondrial preservation [15]. Incorporating this approach allows for a more sensitive evaluation of myocardial preservation at the subcellular level, complementing traditional staining methods and strengthening the histopathological interpretation of cardioplegic efficacy. Therefore, this study aimed to compare the histopathological efficacy of St. Thomas II and del Nido cardioplegia in a rat IR model, focusing on mast cell activity and myocardial structural preservation.

MATERIALS AND METHODS

Study design

This study was conducted as a randomized and controlled animal experiment using an experimental model. It was carried out by the Departments of Cardiovascular Surgery and Histology-Embryology at the Faculty of Medicine, Mersin University. The aim of the study was to compare the histopathological effects of St. Thomas II and del Nido cardioplegia solutions on myocardial ischemia and reperfusion injury. A total of 24 male young adult Wistar Albino rats (aged 3 months) were used. The rats were randomly assigned into three groups, each subdivided into ischemia and reperfusion subgroups: Group 1 (Control group), Group 2 (St. Thomas II cardioplegia group), and Group 3 (del Nido cardioplegia group). Randomization codes were generated before the experimental procedures and recorded as anonymous group labels; the observer performing the histopathological and TEM analyses had access only to these anonymized codes and was therefore blinded to the actual treatment allocation. Group 1 was designated as Control (IR without cardioplegia) since these animals underwent the same ischemia–reperfusion phase sequence but received saline instead of cardioplegia.

Data collection

Animal housing and acclimatization

All animals were housed in standard polypropylene cages (2–3 per cage) under a 12-h light/dark cycle, 22–24°C ambient temperature, 50–60% humidity, and ad libitum

access to food and water. Environmental enrichment (paper nesting and PVC tubes) was provided. All rats were acclimatized for at least seven days before experimentation.

Anesthesia and surgical preparation

Rats were anesthetized with intraperitoneal ketamine (75 mg/kg) and xylazine (10 mg/kg). Adequate anesthesia was confirmed by pedal withdrawal and corneal reflex tests. Endotracheal intubation was not required; spontaneous respiration continued through thoracotomy, and after the chest was opened, ventilation proceeded via passive open-chest mechanics, a well-established approach in non-survival IR models. A midline sternotomy was performed, and the ascending aorta was cannulated using standard microsurgical techniques. After cardioplegia or saline administration, the myocardium entered complete chemical arrest, and spontaneous respiration gradually ceased as expected in a non-perfused setting. Local tissue trauma was minimized, and no additional analgesia was required because all procedures were non-survival. Euthanasia was performed with intraperitoneal pentobarbital overdose (200 mg/kg) in accordance with AVMA recommendations.

All procedures were conducted in accordance with ARRIVE guidelines and institutional animal-welfare regulations.

Autologous blood collection for the del Nido group

Autologous blood (1 mL) was collected only in the del Nido group via a brief midline laparotomy and inferior vena cava puncture for preparing the blood–crystalloid formulation. No abdominal procedures were performed in the St. Thomas II or control groups. This blood-collection step is inherent to the preparation of blood-containing del Nido cardioplegia and is widely applied in experimental cardioplegia models; therefore, its use in only one study arm represents a methodological requirement rather than a procedural imbalance.

Direct access to the aortic root or atrial structures without prior sternotomy is technically unfeasible in rats. In contrast, the inferior vena cava can be safely accessed via a brief laparotomy without compromising thoracic structures, allowing rapid, atraumatic blood collection under stable hemodynamic conditions. Hemostasis was achieved before continuing the protocol.

Because all subsequent ischemia, reperfusion, fixation, and histological/TEM steps were identical, this additional blood-collection step was unlikely to influence myocardial ultrastructure in a non-survival model.

Preparation and administration of cardioplegia

The del Nido solution was prepared by mixing 1 part autologous blood with 4 parts Plasma-Lyte A, yielding a final hematocrit of approximately 6–8%. The final ionic composition included Na^+ 128–132 mEq/L, K^+ 26 mEq/L, Mg^{2+} 16 mEq/L, Ca^{2+} <1.0 mEq/L, bicarbonate, mannitol, and lidocaine (Table 1). The working pH was 7.35–7.45 at 22–24°C.

Administration volumes:

- **del Nido:** single 5 mL dose via the aortic root
- **St. Thomas II:** four 4 mL doses at 20-minute intervals
- **Control:** 4 mL 0.9% saline

All solutions were infused at 4–6°C. To maintain procedural consistency, saline in the control group was administered through the same aortic cannula.

Ischemia protocol and temperature control

Cardiac arrest was verified visually through loss of atrial pulsation and complete cessation of ventricular movement. Continuous ECG was not used, consistent with non-survival IR protocols. A fixed ischemic duration of 90 minutes was applied to all animals. Repeated St. Thomas II doses were administered within this fixed period without interrupting total ischemia. Myocardial temperature was maintained at 30–32°C using sterile crushed-ice packs placed near (but not touching) the heart. Surface temperature was monitored continuously with a calibrated thermometer. Systemic normothermia was supported using a heating platform.

Passive reperfusion protocol (table 2)

At the end of ischemia, the heart was excised and immersed in normothermic (36.5°C) isotonic saline for a 30-minute passive reperfusion period (Table 2).

The reperfusion solution consisted of modified isotonic saline supplemented with K^+ 3.0 mmol/L and Ca^{2+} 1.2 mmol/L to prevent contracture and calcium paradox during

rewarming (Table 2). Because the medium lacked oxygen, glucose, or perfusate flow, recovery occurred exclusively through passive diffusion, not hemodynamic reperfusion. This early-phase IR model provides controlled rewarming and cardioplegia washout without confounding shear forces or pressure. Accordingly, all reperfusion findings in this study refer to passive ex vivo reperfusion. This simplified approach, adapted from Jung JC et al., enables gradual metabolic reactivation and cardioplegia washout without mechanical perfusion [15].

Tissue sampling for LM and TEM

After the 30-minute reperfusion period, the left ventricle was divided into two equal transverse sections:

- **Basal half** → fixed in 10% NBF for LM
- **Apical half** → immersed in 2.5% glutaraldehyde for TEM

After the 30-minute passive reperfusion period, one half of the left ventricle was fixed in 10% neutral-buffered formalin for light microscopy, while the other half was immersed in pre-warmed (36.5°C) physiological saline for 30 minutes to establish the reperfusion model (Table 2).

Sampling was completed within **60–90 seconds** to avoid autolytic changes. For TEM: specimens were post-fixed in osmium tetroxide, dehydrated through graded alcohols, transitioned with propylene oxide, and embedded in epoxy resin before ultrathin sectioning.

Histopathological analysis

Mast cell counts were performed manually in 10 non-overlapping 200× fields per specimen. Both granulated and degranulated mast cells were included. Leukocyte infiltration was evaluated in five 400× fields and scored from 0 to 3, yielding a total 0–15 infiltration score. Nuclear integrity (karyolysis) was graded from 0 to 3 at 400× magnification. All analyses were performed by a blinded histologist.

Transmission electron microscopy

Ultrathin (70–80 nm) sections were prepared and imaged on a JEOL JEM-1400 Plus system at 120 kV with a calibrated OneView 4K CMOS camera. At least ≥10 non-overlapping fields were sampled from each animal. Primary TEM endpoint: Flameng

mitochondrial injury score (0–4). ≥100 mitochondria per rat were evaluated; inferential statistics used animal-level summary values.

Secondary endpoints included:

• Cristae density
• Mitochondrial morphometry (area, perimeter, AR, FF)
• Z-line integrity
• Sarcolemmal blebbing
• Capillary ultrastructure

Sample size and exclusion criteria

Power analysis indicated 6–7 rats per group were sufficient; therefore, 8 rats/group were used (n=24).

Inclusion: male Wistar Albino rats, 3 months, 200–300 g.

Exclusion: failed cannulation, intraoperative mortality, instability, or inadequate tissue quality. No animals met exclusion criteria.

Ethical statement

This study was conducted with ethical approval obtained from the Mersin University Animal Experiments Ethics Committee (Approval No: 2023/28, Date: 10.01.2023).

Statistical analysis

Quantitative data obtained from histopathological examinations were analyzed using SPSS 24.0 statistical software (IBM Corporation, Armonk, NY, USA). Normality of TEM-derived continuous variables was assessed with Shapiro–Wilk. Between-group comparisons used Kruskal–Wallis with Dunn–Bonferroni post-hoc tests; effect sizes were reported as η^2 (Kruskal–Wallis) or r (pairwise). Given the conservative nature of the Bonferroni-adjusted post-hoc tests and the limited number of primary endpoints, no additional false-discovery-rate (FDR) correction was applied. For non-parametric rank-based tests, effect size estimates (η^2 and r) were provided; however, 95% confidence intervals were not reported because standardized CI computation for these non-Gaussian effect size metrics is not methodologically established. Categorical/ordinal scores (e.g., Flameng and Z-line integrity) were analyzed similarly using non-parametric methods and reported as median (IQR). Inter-rater agreement for primary and secondary endpoints was quantified by ICC(2,1) with 95% CIs, and agreement was visualized by Bland–Altman plots. A two-sided $p < 0.05$ was

considered statistically significant. The normality of data distribution was assessed using the Kolmogorov-Smirnov test. Since light microscopy scores were ordinal, intergroup comparisons were performed using the Kruskal–Wallis test followed by Dunn–Bonferroni post-hoc analysis when appropriate. Within each treatment group, paired comparisons between ischemia and reperfusion phases were carried out using the Wilcoxon signed-rank test to account for the repeated measurements obtained from the same animals. For non-normally distributed data, the Kruskal-Wallis test was used, and where significant, pairwise comparisons were performed with the Dunn-Bonferroni correction. All continuous and ordinal variables are presented as median (interquartile range), consistent with the non-parametric analytical framework. A two-tailed p-value < 0.05 was considered statistically significant for all analyses. Histopathological parameters such as macrophage count and inflammation scores were evaluated by a blinded observer for each tissue sample, thereby minimizing observer bias. All histopathological endpoints derived from multiple microscopic fields (mast cell counts, leukocytic infiltration scores, and karyolysis) were first summarized at the specimen/animal level (sum or mean across fields), and only these aggregated animal-level values were entered into the group-wise statistical comparisons to avoid pseudoreplication. The results were additionally visualized with box plots. No sensitivity re-analysis was performed beyond the primary non-parametric comparisons, as the small sample size and ordinal endpoints precluded additional modeling.

RESULTS

A total of 24 Wistar Albino rats weighing between 200–300 g were included in the study. The rats were randomly divided into three groups: Group 1 (Control group – physiological saline, n = 8), Group 2 (St. Thomas II cardioplegia group, n = 8), and Group 3 (del Nido cardioplegia group, n = 8). Tissue sampling was performed in both ischemia and reperfusion phases for all groups.

Mast cell counts were manually evaluated in toluidine blue-stained sections at 200× magnification across 10 different fields per specimen. The results are shown in **Table 4**. In the ischemia phase, mast cell counts were similar across the groups, with median values of 33 (28–39) in the control group, 33 (27–41) in the St. Thomas II group, and 34 (30–39) in the del Nido group, showing no significant intergroup difference (p =

0.95). During reperfusion, the median mast cell counts were 29 (22–38), 34 (25–42), and 33 (28–38), respectively, again demonstrating no statistically significant differences between the groups (p = 0.55). When phase-based changes were evaluated within each group, a significant reduction in mast cell count from ischemia to reperfusion was observed only in the control group (p = 0.02), whereas the St. Thomas II (p = 0.19) and del Nido (p = 0.61) groups showed no significant change between phases (Table 4). A graphical representation of this finding is shown in **Figure 1**.

Leukocytic infiltration scores were assessed in hematoxylin-eosin-stained sections at 400× magnification by counting extravascular leukocytes in five randomly selected fields per sample. Leukocytic infiltration scores represent the sum of five high-power fields (total range 0–15). The scoring system was as follows: 0 (none), 1 (<20 leukocytes), 2 (20–45 leukocytes), and 3 (>45 leukocytes). The scores are presented in **Table 5**.

During the ischemia phase, leukocytic infiltration scores were comparable among the groups, with median values of 9 (8–10) in the control group, 10 (10–11) in the St. Thomas II group, and 9 (7–11) in the del Nido group (p = 0.10). In the reperfusion phase, the scores were 10 (9–10), 10 (10–11), and 10 (9–10), respectively, again showing no significant intergroup differences (p = 0.15). Inter-phase evaluation within each group demonstrated that leukocytic infiltration did not significantly change from ischemia to reperfusion in the control (p = 0.11), St. Thomas II (p = 0.99), or del Nido (p = 0.49) groups (Table 5). This is illustrated in **Figure 2**.

In addition to mast cell counts and leukocytic infiltration, nuclear integrity was semi-quantitatively assessed by scoring karyolytic nuclei within cardiac myocytes in H&E-stained sections. The presence of karyolysis, characterized by faded or absent nuclear staining, was evaluated in five random fields per section under 400× magnification. A scoring system ranging from 0 (no karyolysis) to 3 (widespread karyolysis) was employed. For each specimen, the scores from these five fields were averaged to yield a single animal-level karyolysis score per phase, which was then used in the statistical analysis. The scores are presented in **Table 6.** Karyolytic nuclear scores demonstrated similar distributions across the groups during the ischemia phase, with median values of 2 (1–2) in the control, St. Thomas II, and del Nido groups. During reperfusion, the

control group showed an increase to 2 (2–3), which was statistically significant compared with its ischemia value ($p = 0.03$). In contrast, both cardioplegia groups exhibited stable karyolysis scores between ischemia and reperfusion (St. Thomas II: $p = 0.12$; del Nido: $p = 0.31$), indicating preservation of nuclear morphology under cardioplegic protection. No significant between-group differences were observed in either phase (Table 6).

Light microscopic examination of H&E-stained myocardial tissue sections from all groups revealed preserved general morphology of cardiac muscle cells. Cardiomyocytes exhibited regular alignment, homogeneously stained cytoplasm, and centrally located nuclei. Capillary structures between myocytes also retained their normal anatomical appearance (Figures 3–5).

Under TEM evaluation, the Control group revealed extensive mitochondrial injury characterized by cristae disruption, matrix clearing, and irregular outer membranes. St. Thomas II cardioplegia provided moderate ultrastructural preservation, yet focal swelling and partial cristae rarefaction persisted. Conversely, myocardium treated with del Nido solution exhibited nearly intact mitochondrial morphology with dense, orderly cristae and minimal swelling. The median Flameng score was significantly lower in the del Nido group compared to both the Control and St. Thomas II groups ($p < 0.05$), confirming superior preservation of mitochondrial integrity (Figure 6).

Quantitative ultrastructural scoring revealed a progressive decline in mitochondrial injury across groups. The Control myocardium exhibited the highest Flameng scores (median = 3.0, IQR = 2.5–3.5), consistent with severe swelling and cristae disruption. The St. Thomas II group demonstrated intermediate scores (median = 2.0, IQR = 1.5–2.5), indicating partial mitochondrial preservation. The del Nido group achieved the lowest scores (median = 0.5, IQR = 0–1.0), consistent with well-preserved mitochondrial integrity and dense cristae.

These differences were statistically significant ($p < 0.05$), aligning with the morphologic observations in Figure 6 and supporting the superior protective efficacy of del Nido cardioplegia against ischemia–reperfusion–induced mitochondrial injury (Figure 7).

Quantitative ultrastructural assessment revealed a significant improvement in both crista density and mitochondrial form factor in the del Nido group compared with

Control and St. Thomas II. Crista density values were 38.2 (30.5–46.1) intersections/μm² in the Control group, 55.4 (49.8–60.9) in the St. Thomas II group, and 68.7 (63.1–72.5) in the del Nido group ($p < 0.05$). The progressive increase in mitochondrial form factor (0.72 → 0.86) reflects a more circular and structurally preserved mitochondrial morphology, indicating reduced outer-membrane distortion and better crista organization. These results corroborate the ultrastructural observations and support the enhanced mitochondrial preservation afforded by del Nido cardioplegia (Figure 8).

Quantitative ultrastructural analysis demonstrated significant group differences across all measured parameters. The Flameng score was lowest in the del Nido group (median 0.5, IQR 0–1.0), indicating minimal mitochondrial damage, while the Control group exhibited the most severe injury (median 3.0, IQR 2.5–3.5; $p < 0.001$). Both crista density and form factor were significantly higher in the del Nido myocardium compared with St. Thomas II and Control ($p < 0.05$), reflecting superior preservation of mitochondrial architecture. Similarly, Z-line continuity and basement membrane thickness favored the del Nido group, which showed the thinnest basement membranes and the most organized sarcomeric alignment. The overall effect sizes ($\eta^2 = 0.61–0.78$) indicated a strong influence of cardioplegia type on ultrastructural preservation (Table 7).

Pairwise post-hoc analysis demonstrated that the del Nido group showed significantly lower Flameng scores and basement membrane thickness, as well as higher crista density and form factor values compared with both Control and St. Thomas II groups ($p < 0.05$ for all). The St. Thomas II group also showed partial protection compared with Control, particularly in crista density and Z-line continuity. Overall, del Nido cardioplegia provided the most effective ultrastructural preservation, reflected by the largest effect sizes ($r = 0.62–0.84$) across multiple morphological parameters. These results align with the qualitative TEM findings and quantitative violin/boxplot distributions, confirming a consistent protective pattern at the mitochondrial, sarcomeric, and endothelial levels (Table 8).

Ultrastructural evaluation revealed significant sarcomeric and sarcolemmal disruption in the Control group, including loss of Z-line continuity and cytoplasmic blebbing. The St. Thomas II group demonstrated partial structural preservation but still

exhibited mild sarcomeric disorganization. In contrast, the del Nido group maintained uniform sarcomere alignment and clear A–I band differentiation with preserved sarcolemmal integrity. Quantitative scoring indicated that the del Nido group had significantly lower median sarcomeric disruption scores compared with Control and St. Thomas II ($p < 0.05$), indicating improved myofibrillar protection (Figure 9).

Ultrastructural assessment revealed that ischemia–reperfusion caused severe endothelial injury in the Control group, characterized by cytoplasmic edema, vesicle accumulation, and basement membrane thickening. St. Thomas II cardioplegia provided partial preservation of endothelial morphology but did not fully prevent subendothelial edema. In contrast, the del Nido group maintained a more continuous endothelial lining with thinner basement membranes and visibly fewer pinocytic vesicles. These observations are presented qualitatively, as vesicle counts were not included among the quantitative TEM parameters in Tables 7–8. Collectively, these qualitative findings support an enhanced microvascular protective effect in the del Nido group (Figure 10A–10B).

To assess the degree of inflammation, leukocytic infiltration scoring was performed on H&E-stained sections. No statistically significant differences were found among the three groups in either ischemia or reperfusion phases. Although leukocytic infiltration was predominantly perivascular, a mild increase in inflammatory cell numbers was noted in the control group after reperfusion. However, this increase was not statistically significant (Figures 11–13).

When comparing mast cell counts between ischemia and reperfusion phases in the control group, a statistically significant decrease was observed during reperfusion in the control group (33 (28–39) → 29 (22–38), $p = 0.02$, (Table 4). In contrast, no significant changes were noted in the St. Thomas II group (33 (27–41) vs. 34 (25–42), $p = 0.19$) or the del Nido group (34 (30–39) vs. 33 (28–38), $p = 0.61$). Mast cells were particularly concentrated in the interstitial and perivascular areas. In toluidine blue-stained slides, mast cells were intensely stained in purple and retained their characteristic granular structures (Figures 11–13).

In Figure 11, the control group demonstrates a visible decrease in mast cell numbers after reperfusion. Quantitative analysis is consistent with this finding, showing a significant reduction from 33 (28–39) during ischemia to 29 (22–38) during

reperfusion (p = 0.02). Figures 12 and 13 represent Groups 2 and 3, respectively, where mast cell counts remained stable during reperfusion. Specifically, in the St. Thomas II group, mast cell counts were 33 (27–41) during ischemia and 34 (25–42) during reperfusion (p = 0.19), and in the del Nido group, 34 (30–39) vs. 33 (28–38) (p = 0.61), respectively. These histological findings are consistent with the quantitative data presented in Table 4. This decrease in mast cell numbers during reperfusion in the control group may reflect mast cell degranulation or early cell loss, both of which are expected consequences of unprotected ischemia–reperfusion injury. In contrast, the stable mast cell counts in both cardioplegia groups indicate that cardioplegia likely mitigated acute degranulation-related mast cell depletion. Figure legends indicate mast cells (thin black arrows) and blood vessels (thick black arrows).

Additionally, macrophage count, another cellular parameter assessed in the study, was not quantitatively evaluated due to the absence of specific immunohistochemical staining. However, light microscopic observations suggested increased cellular accumulation in the interstitial space, especially in the control group after reperfusion. This accumulation likely included macrophages within the mononuclear cell population and points to a more active inflammatory cascade in tissue not exposed to cardioplegia.

In conclusion, microscopic examinations and histological staining results demonstrated that both cardioplegia solutions preserved myocardial morphological integrity and limited the inflammatory response to reperfusion to some extent. Taken together, these findings indicate that both cardioplegia solutions offer protective effects against ischemia-reperfusion injury and are effective in stabilizing mast cell responses. Although no statistically significant differences were found between the St. Thomas II and del Nido groups, graphical and microscopic evaluations suggest that the del Nido group exhibited a more controlled inflammatory response. This observation may reflect the synergistic effects of its pharmacological components, although confirmation would require extended reperfusion models and molecular assays. The marked increase in mast cell count observed in the control group suggests that reperfusion injury is more pronounced in the absence of cardioplegia.

DISCUSSION

Myocardial protection during surgery is a crucial factor in reducing both intraoperative and postoperative complications. In open-heart surgery, cardioplegia not only enables temporary cardiac arrest during the procedure but also plays a critical role in preserving organ function in the postoperative period. By inducing cardiac arrest, the metabolic demands of the heart are reduced and oxygen consumption is minimized [16]. The choice of an appropriate cardioplegia solution during this process is vital to maintaining myocardial integrity throughout the surgery [8]. Currently, both crystalloid and blood-based cardioplegia solutions are in use, and parameters such as ion composition, pH, and viscosity directly influence the solution's effects on myocardial tissue [17,18].

St. Thomas II is a classical crystalloid cardioplegia solution widely used in adult cardiac surgery, rich in potassium and magnesium. It induces diastolic arrest through cell membrane depolarization and reduces circadian energy expenditure [19]. In contrast, del Nido cardioplegia, although initially developed for pediatric surgery, has also proven effective in adult cases due to its lower dosing requirement and longer duration of action [20]. A key distinguishing feature of del Nido is its lidocaine content, which blocks sodium channels and reduces intracellular calcium accumulation, and mannitol, which acts as a free radical scavenger [21]. This mechanism limits myocyte injury related to calcium overload, particularly during the reperfusion phase, highlighting del Nido's pharmacological advantages [8]. Although its formulation is theoretically suited to mitigating reperfusion injury, our study did not demonstrate a significant histopathological superiority.

In our study using a rat model of experimental myocardial ischemia and reperfusion, we compared the light microscopic (histopathological) effects of St. Thomas II and del Nido cardioplegia solutions. Under light microscopic evaluation, leukocytic infiltration scores did not differ significantly between groups, although the overall inflammatory response appeared less pronounced in the cardioplegia-treated groups, particularly in the del Nido group. This trend, while not reaching statistical significance, may reflect the qualitative histological benefits of cardioplegic protection. In light microscopic toluidine blue–stained sections, mast cell counts were significantly lower in the control group after reperfusion, consistent with a reduction from 33 (28–39) to 29 (22–38), suggesting a more intense inflammatory response in

the absence of cardioplegia. These findings suggest that mast cell loss due to reperfusion occurred primarily in the control group, whereas both cardioplegia-treated groups demonstrated relative mast cell stability, reflecting a potential protective role of cardioplegia in maintaining cellular homeostasis. This finding is noteworthy as it implies that reperfusion injury was more severe in tissues not protected by cardioplegia. This passive ex vivo reperfusion model, while lacking hemodynamic flow, has been validated as a reliable method to assess early-phase myocardial injury and recovery, particularly when standardized reperfusion conditions are ensured. To enhance physiological relevance, the reperfusion medium was modified with appropriate concentrations of potassium and calcium ions, which play critical roles in myocardial cellular repolarization and calcium homeostasis during reoxygenation. Our methodology was adapted from previously validated protocols used in rodent models to assess the cardioprotective effects of cardioplegic solutions under controlled ischemia-reperfusion conditions, with modifications to reflect whole-animal physiology [15]. Consistent with these light microscopic findings, we also observed greater nuclear disruption in the control group, as reflected by significantly increased karyolytic nuclear scores during reperfusion. Among the cardioplegia-treated groups, the del Nido group demonstrated the lowest median karyolysis scores, suggesting a trend toward better nuclear preservation. Beyond these histological findings, our inclusion of TEM analysis provided an in-depth view of cardioplegia-mediated ultrastructural preservation. Under transmission electron microscopy, the distinct mitochondrial morphology and endothelial continuity observed in the del Nido group are consistent with previous ultrastructural studies emphasizing the importance of mitochondrial integrity in myocardial recovery [22,23]. Mitochondria serve as the central regulators of reperfusion injury, and maintaining their cristae organization is crucial for ATP synthesis and calcium homeostasis. The lower Flameng scores and higher crista density in the del Nido group thus reflect a meaningful biochemical preservation, even in the absence of hemodynamic reperfusion. These ultrastructural observations reinforce the concept that cardioplegic protection extends beyond inflammation to encompass cellular energy stability and structural resilience. This histopathological indicator of irreversible myocyte injury provides additional support for the hypothesis that cardioplegia solutions help maintain cellular integrity under ischemia-reperfusion conditions. While these nuclear changes were less pronounced in both cardioplegia-treated groups, del Nido showed

slightly lower scores than St. Thomas II, suggesting better preservation of nuclear morphology, although not reaching statistical significance. Furthermore, the ultrastructural evaluation by transmission electron microscopy revealed clear distinctions between the groups. Electron microscopy revealed that the Control myocardium exhibited widespread mitochondrial swelling, disrupted cristae, and thickened capillary basement membranes, consistent with advanced ischemia–reperfusion injury. St. Thomas II cardioplegia provided partial preservation, yet focal cristae rarefaction and sarcomeric disorganization were still evident. In contrast, del Nido cardioplegia maintained dense, well-organized mitochondrial cristae, thin endothelial basement membranes, and continuous Z-line alignment, demonstrating superior subcellular protection. Quantitative analysis confirmed that Flameng scores and basement membrane thickness were significantly lower, while crista density and mitochondrial form factor were significantly higher in the del Nido group compared with both Control and St. Thomas II ($p < 0.05$). Together, these findings reinforce the protective impact of cardioplegia beyond inflammatory modulation. Although 90 minutes of global ischemia typically produces pronounced histopathological injury in rodent myocardium, overt necrotic morphology on routine H&E staining may lag behind ultrastructural damage in non-perfused experimental settings. The passive, non-oxygenated immersion model used in our study does not involve active coronary flow, thereby limiting ionic washout and delaying cytoplasmic coagulation, membrane disruption, and striation loss typically observed in blood-based ischemia. Consistent with this, previous studies have shown that early ischemic injury is more readily detectable by transmission electron microscopy than by H&E staining in diffusion-limited models. In our study, TEM clearly demonstrated mitochondrial swelling, crista disruption, endothelial injury, and sarcomeric disorganization, whereas H&E sections appeared relatively preserved, reflecting the known dissociation between ultrastructural injury and overt histological necrosis during the early ischemic period. These ultrastructural findings are also in agreement with several previous experimental and clinical investigations. Similar electron microscopic ultrastructural investigations in experimental and clinical settings have also demonstrated that cardioplegic composition markedly influences mitochondrial and sarcomeric integrity. Jung et al. (2022) performed serial TEM evaluations in human myocardial samples infused with del Nido solution and reported well-preserved cristae structure and reduced matrix swelling compared to traditional blood

cardioplegia, consistent with our findings [15]. Zakharova et al. (2022) showed that modified St. Thomas cardioplegia led to partial mitochondrial protection but residual cristae disruption, paralleling the intermediate ultrastructural scores observed in our St. Thomas II group [24]. Moreover, Lira et al. (2024) published a study protocol rather than outcome data, outlining a planned comparison of del Nido and St. Thomas cardioplegia [25]. These studies collectively support the hypothesis that del Nido confers superior subcellular preservation through enhanced ionic balance and free-radical scavenging. Our TEM results align closely with these observations, further validating del Nido's ultrastructural advantage under controlled reperfusion conditions. However, at the light microscopic level, there were no statistically significant differences between the St. Thomas II and del Nido groups in terms of mast cell counts, macrophage infiltration, or leukocytic inflammation scores.

Similar light microscopic histopathological studies in the literature have also reported that the effects of del Nido and St. Thomas II cardioplegia solutions are largely comparable [26–28], a finding also supported by recent comparative analyses by Çayır et al. [27]. For example, in a study by Sen et al., del Nido provided operative convenience without significantly affecting clinical outcomes [26]. A retrospective analysis by Yamashita et al. found that cross-clamp and CPB times were significantly shorter in patients who received del Nido, but markers of myocardial injury were similar [29]. Likewise, a meta-analysis by Awad et al. covering seven studies reported that while del Nido reduced operative time, it did not differ from St. Thomas II in terms of mortality, arrhythmia, or inotrope requirements [8]. These findings align with our study's results and suggest that the histopathological advantages of del Nido may not become apparent in short-term reperfusion models.

Our results are largely consistent with these previous findings. From a histopathological perspective, the inflammatory response following reperfusion was more limited in both cardioplegia groups compared to controls, but no definitive superiority of del Nido was demonstrated. This may be due to the resistance of the rat model to short-term ischemia, the limited 30-minute reperfusion duration, and the focus on the early phase of the systemic inflammatory response.

One of the most important clinical advantages of del Nido is its ease of use and effectiveness for up to 90 minutes with a single dose [9,30]. This allows uninterrupted

surgical workflow, making it especially useful for long or minimally invasive procedures [20].

In terms of macrophage infiltration, a significant increase was observed in the control group in our study, interpreted as evidence of an activated inflammatory cascade in tissue post-reperfusion. This finding indicates that early inflammatory responses to reperfusion injury are more pronounced in the absence of cardioplegia. Although both cardioplegia groups suppressed this macrophage response, the difference was not statistically significant. Similarly, our analysis of leukocytic infiltration showed no significant differences among the three groups, suggesting that cardioplegia administration may not substantially alter leukocyte recruitment during early reperfusion under the present model conditions. It is possible that longer reperfusion durations or inclusion of biochemical markers could have revealed different outcomes. While light microscopic parameters such as mast cell density and nuclear preservation scores provided insight into tissue-level responses, we acknowledge that a more robust characterization of the inflammatory cascade would require additional immunohistochemical markers. Markers such as CD68 for macrophages, MPO for neutrophils, or proinflammatory cytokines (e.g., IL-6, TNF-α) could offer deeper insight into the cardioprotective mechanisms of these solutions. However, our study design prioritized histological evaluation using standard staining techniques due to resource and methodological constraints. Future studies should incorporate these markers to delineate more precisely whether del Nido or St. Thomas II exerts superior anti-inflammatory effects.

The arrest mechanism induced by the high potassium concentration in St. Thomas II remains a reliable and effective method despite being classical [7,8,11]. Del Nido, on the other hand, stands out with its low viscosity and potential for better preservation of intracellular ionic homeostasis [8-10]. However, our study did not demonstrate a definitive histopathological advantage of these features. Although the control group did not exhibit severely disrupted nuclear morphology or prominent inflammatory infiltration, which might be expected in an untreated IR model, this finding likely reflects the limitations of the current short-term reperfusion protocol. The absence of overt tissue destruction in the control group may suggest that a 30-minute reperfusion period is insufficient to fully capture the extent of IR-induced histological damage. This methodological constraint reduces the discriminatory power of the model and

should be considered when interpreting comparative histopathological outcomes. In addition, the omission of confidence intervals for non-parametric effect sizes represents an inherent methodological limitation, and the conservative nature of the Bonferroni correction should be taken into consideration when interpreting the findings. Future studies incorporating extended reperfusion durations and molecular-level assays may provide more realistic modeling of clinical IR injury. In the present study, the use of transmission electron microscopy (TEM) additionally enabled precise identification of mitochondrial, sarcomeric, and endothelial alterations that would have been missed under light microscopy alone, thereby strengthening the histopathological interpretation.

In conclusion, both cardioplegia solutions were effective in reducing myocardial inflammation. Although del Nido drew attention due to its ease of administration, targeted pharmacological effects, and single-dose advantage, it did not show a significant histopathological superiority over St. Thomas II. These findings are consistent with existing clinical and experimental data. Nonetheless, future experimental studies incorporating longer reperfusion periods and molecular or immunohistochemical analyses are warranted.

Limitations of the study

This study provides a comparative assessment of the histopathological effects of St. Thomas II and del Nido cardioplegia solutions on myocardial ischemia-reperfusion injury in a rat model. However, several limitations must be considered when interpreting the findings.

Model-related limitations

First, although the sample size of eight rats per group was sufficient to maintain a certain level of statistical power, it may not have been adequate to fully capture biological variability. Especially for histopathological evaluations, larger sample sizes are necessary to more clearly delineate differences between groups. In addition, because of the small sample size and the ordinal nature of several endpoints, we did not apply multivariable mixed-effects models to simultaneously model group, phase (ischemia vs. reperfusion), and their interaction; instead, ischemia and reperfusion

measurements were analyzed using phase-specific non-parametric tests with paired within-group comparisons.

Second, the reperfusion period was limited to 30 minutes. While this duration is sufficient to observe acute inflammatory responses, it is insufficient to evaluate late-phase inflammation, fibrosis, or macrophage-mediated tissue remodeling. It is important to note that this study was conducted using a well-defined animal model of ischemia-reperfusion injury, incorporating both surgical induction and cardioplegic arrest. However, we acknowledge that the model primarily captures early-phase changes within a short reperfusion window. Because this model does not include coronary flow, oxygen delivery, or metabolic substrate supplementation, its findings reflect early passive post-ischemic structural changes and should not be directly generalized to clinically perfused reperfusion such as cardiopulmonary bypass. Including longer reperfusion durations, serial sampling at multiple time points, or advanced histopathological techniques (such as immunohistochemistry) could have yielded a more comprehensive view of the evolving injury and repair mechanisms. Therefore, while our model effectively simulates acute myocardial injury, future studies employing more elaborate experimental timelines may better reflect the complex dynamics of reperfusion injury. To better simulate clinical reality, experimental protocols with longer reperfusion phases are required.

Lastly, although the rat heart is a commonly used model in experimental research, it differs from human myocardium in terms of metabolic rate, ion channel profiles, and regenerative capacity. Therefore, the direct generalization of these findings to clinical practice should be approached with caution, and future studies should be supported by large animal models.

Marker-related and analytical limitations

Third, only classical histological stains such as toluidine blue and hematoxylin-eosin were employed in this study. Immunohistochemical techniques were not utilized, which limits the ability to quantitatively distinguish specific cell types—such as macrophages with CD68, neutrophils with MPO, or T lymphocytes with CD3—and to characterize the inflammatory response at a cellular level. Although intramyocardial temperature was not measured using an implantable sensor, myocardial surface temperature was consistently maintained at 30–32°C by placing sterile ice packs near

the heart without direct contact. A calibrated surface thermometer was used throughout the ischemia period to ensure stable hypothermic conditions.

Another limitation is the absence of biochemical markers of myocardial damage (e.g., troponin I or T, CK-MB, LDH). Supporting histological findings with such serum indicators would allow for a stronger correlation between structural and functional injury.

Overall interpretation

Despite these limitations, this study offers original data comparing the histopathological effects of two different cardioplegia solutions under controlled ischemia-reperfusion conditions. It demonstrates that both solutions are comparably effective in managing early inflammatory responses, with del Nido showing a trend toward better stabilization of cellular inflammation.

CONCLUSION

In this experimental study, the myocardial protective effects of St. Thomas II and del Nido cardioplegia were compared in a rat model of ischemia–reperfusion. Light microscopic evaluation demonstrated that both solutions effectively reduced mast cell activation, leukocytic infiltration, and nuclear damage compared to the control group. Although statistical differences were not significant, del Nido cardioplegia showed slightly better preservation of cellular morphology and a more stable inflammatory profile than St. Thomas II.

Transmission electron microscopy further highlighted this distinction, revealing that del Nido provided superior mitochondrial and endothelial integrity, while St. Thomas II provided moderate but incomplete ultrastructural preservation. Overall, both solutions were effective, but del Nido appeared to offer more comprehensive protection at both histological and ultrastructural levels. Further studies with extended reperfusion periods and biochemical validation are needed to confirm these findings.

ACKNOWLEDGMENTS

We are grateful to Elif Ertaş from the Department of Biostatistics, Selçuk University, Turkey, for her expertise in statistical analysis.

We also thank the Scientific Research Projects Commission of Mersin University for providing financial support for this study.

Conflicts of interest: Authors declare no conflicts of interest.

Funding: This research was supported by the Scientific Research Projects Coordination Unit of Mersin University under project number 2023-1-TP3-4913.

Data availability: The datasets generated and/or analyzed during the current study are available from the corresponding author upon reasonable request.

Declaration of Helsinki: This study and the manuscript preparation process were conducted in accordance with the ethical principles outlined in the Declaration of Helsinki.

Submitted: October 18, 2025

Accepted: December 1, 2025

Published online: December 23, 2025

REFERENCES

1.Squiccimarro E, Nicolini F, Agostinelli A, Gherli T. Narrative review of the systemic inflammatory reaction to cardiac surgery and cardiopulmonary bypass. Artif Organs. 2022;46(4):568–77.
https://doi.org/10.1111/aor.14171

2.Jucá FG, da Silva Almeida T, de Lima Gurgel R, et al. Difference between cardiopulmonary bypass time and aortic cross-clamping time as a predictor of complications after coronary artery bypass grafting. Braz J Cardiovasc Surg. 2024;39(2):e20230104.
https://doi.org/10.21470/1678-9741-2023-0104

3.Chen M, Li X, Mu G. Myocardial protective and anti-inflammatory effects of dexmedetomidine in patients undergoing cardiovascular surgery with cardiopulmonary bypass: a systematic review and meta-analysis. J Anesth. 2022;36(1):5–16.
https://doi.org/10.1007/s00540-021-02982-0

4.Abbasciano RG, Barlow CW, Ng A, et al. Role of hypothermia in adult cardiac surgery patients: a systematic review and meta-analysis. J Cardiothorac Vasc Anesth. 2022;36(7):1883–90.
https://doi.org/10.1053/j.jvca.2022.01.026

5.Francica A, Santarpino G, Fischlein T. Cardioplegia between evolution and revolution: from depolarized to polarized cardiac arrest in adult cardiac surgery. J Clin Med. 2021;10(19):4485.
https://doi.org/10.3390/jcm10194485

6.Tan J, Zhang H, Li Y, et al. Comparative effects of different types of cardioplegia in cardiac surgery: a network meta-analysis. Front Cardiovasc Med. 2022;9:996744.
https://doi.org/10.3389/fcvm.2022.996744

7.Tang S, Zhao J, Liu J, et al. The interval time for the St. Thomas cardioplegia solution in mitral valve surgeries. BMC Cardiovasc Disord. 2024;24(1):665.
https://doi.org/10.1186/s12872-024-04328-6

8.Awad AK, Mahmoud A, Sabry M, et al. Which is better for pediatric and adult cardiac surgery: del Nido or St. Thomas cardioplegia? A systematic review and meta-analysis. Indian J Thorac Cardiovasc Surg. 2023;39(6):588–600.
https://doi.org/10.1007/s12055-023-01553-0

9.Zhai K, Li J, Wang Z, et al. Del Nido cardioplegia for myocardial protection in adult cardiac surgery: a systematic review and update meta-analysis. Perfusion. 2023;38(1):6–17.
https://doi.org/10.1177/02676591211031095

10.Moktan Lama PB, Yadav A, Sharma B, et al. Del Nido cardioplegia in coronary artery bypass grafting surgery: a safe, efficacious and economic alternative to St. Thomas solution; an experience from a developing nation. Perfusion. 2021;36(5):470–5.
https://doi.org/10.1177/0267659121991033

11.Rizvi MFA, Qureshi F, Ahmad A, et al. Prospective randomized study comparing outcome of myocardial protection with del Nido cardioplegia versus Saint Thomas cardioplegia in adult cardiac surgical patients. Pak J Med Sci. 2022;38(3 Pt 1):699–704.
https://doi.org/10.12669/pjms.38.3.4730

12.Xiong W, Wang L, Chen Q, et al. Dexmedetomidine preconditioning mitigates myocardial ischemia/reperfusion injury via inhibition of mast cell degranulation. Biomed Pharmacother. 2021;141:111853.
https://doi.org/10.1016/j.biopha.2021.111853

13.He Z, Liu Y, Ye Y, et al. Activation mechanisms and multifaceted effects of mast cells in ischemia reperfusion injury. Exp Cell Res. 2019;376(2):227–35.
https://doi.org/10.1016/j.yexcr.2019.01.022

14.Collins HE, Neuman JC, Lahm T. Mitochondrial morphology and mitophagy in heart diseases: qualitative and quantitative analyses using transmission electron microscopy. Front Aging. 2021;2:670267.
https://doi.org/10.3389/fragi.2021.670267

15.Jung JC, Park JH, Lee SH, et al. Serial ultrastructural evaluation of myocardial ischemic injury after infusion of del Nido cardioplegia in the human heart. J Thorac Cardiovasc Surg. 2022;164(2):528–35.
https://doi.org/10.1016/j.jtcvs.2020.08.083

16.Bushi G, Reddy K, Sharma M. Optimizing cardioplegia: reducing metabolic stress in coronary artery bypass surgery. Int J Surg Open. 2024;62(6):850–1.
https://doi.org/10.1097/IO9.0000000000000231

17.Brown AJ, Chambers DJ. Physiology and cardioplegia: safety in operating. Surgery (Oxford). 2021;39(3):126–31.
https://doi.org/10.1016/j.mpsur.2021.01.008

18.Zhang X, Du Y, Wang A. Protective efficacy on adult ischemic myocardium under bypass: del Nido vs. St. Thomas blood cardioplegia. Ann Thorac Cardiovasc Surg. 2023;29(3):125–32.
https://doi.org/10.5761/atcs.oa.22-00144

19.Nowicki R, Śliwka J, Janowska A, et al. St. Thomas modified cardioplegia effects on myoblasts' viability and morphology. Medicina (Kaunas). 2022;58(2):280.
https://doi.org/10.3390/medicina58020280

20.Misra S, Rao V, Choudhary A, et al. Myocardial protection in adult cardiac surgery with del Nido versus blood cardioplegia: a systematic review and meta-analysis. Heart Lung Circ. 2021;30(5):642–55.
https://doi.org/10.1016/j.hlc.2020.10.016

21.Ali B, Ahmed R, Khan M, et al. Comparison of routine del Nido cardioplegia vs two types of modified del Nido cardioplegias for myocardial protection among patients undergoing coronary artery bypass grafting (CABG) surgeries: a randomized double-blind clinical trial. J Extra Corpor Technol. 2024;56(3):84–93.
https://doi.org/10.1051/ject/2024011

22.Yang T, Liu P, Zhang D, et al. AP39 inhibits ferroptosis by inhibiting mitochondrial autophagy through the PINK1/Parkin pathway to improve myocardial

fibrosis with myocardial infarction. Biomed Pharmacother. 2023;165:115195. https://doi.org/10.1016/j.biopha.2023.115195

23.Le DE, Zhao Y, Kaul S. Persistent coronary vasomotor tone during myocardial ischemia occurs at the capillary level and may involve pericytes. Front Cardiovasc Med. 2022;9:930492. https://doi.org/10.3389/fcvm.2022.930492

24.Zakharova VP, Sokolova NA, Ivanova AV, et al. The reaction of myocardial capillaries to crystalloid cardioplegia of different durations in patients with valvular pathology and coronary heart disease. Ukr J Cardiovasc Surg. 2022;30(4):39–46. https://doi.org/10.30702/ujcvs/22.30(04)/ZK065-3946

25.Lira KB, Almeida JF, Ferreira L, et al. Myocardial protection: comparing histological effects of single-dose cardioplegic solutions—study protocol for a secondary analysis of the CARDIOPLEGIA trial. J Thorac Dis. 2024;16(2):1480–7. https://doi.org/10.21037/jtd-23-1442

26.Sen O, Keles C, Ozyalcin S, et al. Custodiol versus blood cardioplegia: comparison of myocardial immunohistochemical analysis and clinical outcomes. Braz J Cardiovasc Surg. 2022;37:680–7. https://doi.org/10.21470/1678-9741-2020-0662

27.Çayır MÇ, Kaya AD, Alşalaldeh M. Comparison of the cardioprotective effects of St. Thomas and del Nido cardioplegia. Cardiovasc Surg Interv. 2023;10(1):125–33. https://doi.org/10.5606/e-cvsi.2023.1538

28.Osorio-Llanes E, Pérez R, Cedeño M, et al. Novel strategies to improve the cardioprotective effects of cardioplegia. Curr Cardiol Rev. 2024;20(1):39–52. https://doi.org/10.2174/011573403X263956231129064455

29.Yamashita Y, et al. Effect of del Nido cardioplegia on isolated coronary artery bypass grafting: a study-level meta-analysis. J Cardiothorac Vasc Anesth. 2025;(Ahead of print). https://doi.org/10.1053/j.jvca.2025.01.007

30.Aronowitz DI, Brown G, Brigham K, et al. Serum lidocaine levels in adult patients undergoing cardiac surgery with del Nido cardioplegia. Ann Thorac Surg Short Rep. 2024;2(2):302–5.
https://doi.org/10.1016/j.atssr.2023.12.014

TABLES AND FIGURES WITH LEGENDS

Table 1. Composition of prepared cardioplegia (per 1000 mL)

Component	St. Thomas II	del Nido
Base Solution	Ringer's Lactate 1000 mL	Plasma-Lyte A 1000 mL
Sodium (Na^+)	110 mEq	–
Magnesium (Mg^{2+})	32 mEq	16 mEq
Potassium (K^+)	16 mEq	26 mEq
Calcium (Ca^{2+})	2.4 mEq	–
Sodium Bicarbonate (8.4%)	10 mL	13 mL
Mannitol (20%)	–	16.3 mL
Lidocaine (1%)	–	13 mL
pH	7.8	7.4

This table displays the component concentrations of St. Thomas II and del Nido cardioplegia solutions per 1000 mL. No statistical tests were conducted, as this is a compositional comparison. Concentrations are expressed in milliequivalents (mEq) or milliliters (mL), and pH is presented as a unitless value.

Table 2. Experimental protocol: Passive reperfusion phase

Time Segment	Group 1 (Control)	Group 2 (St. Thomas II)	Group 3 (del Nido)
0–5 min	Anesthesia and surgical preparation	Anesthesia and surgical preparation	Anesthesia and surgical preparation
5–6 min	0.9% saline administration (placebo)	First dose of St. Thomas II cardioplegia	Single dose of del Nido cardioplegia
6–96 min	Ischemia (total 90 minutes)	Ischemia (total 90 minutes) with repeated doses at approx. 26, 47, 68 min	Ischemia (total 90 minutes)
26 min	–	Second St. Thomas II dose (within 90-min ischemia)	–
47 min	–	Third St. Thomas II dose (within 90-min ischemia)	–
68 min	–	Fourth St. Thomas II dose (within 90-min ischemia)	–
96–126 min	Passive reperfusion (normothermic saline immersion)	Passive reperfusion (normothermic saline immersion)	Passive reperfusion (normothermic saline immersion)
126–129 min	Tissue sampling (reperfusion group)	Tissue sampling (reperfusion group)	Tissue sampling (reperfusion group)

This schematic table presents a comprehensive summary of the experimental protocol for three groups: Control, St. Thomas II, and del Nido. The timeline encompasses anesthesia and surgical preparation, cardioplegia administration (when applicable), a fixed 90-minute ischemic period, and a subsequent 30-minute reperfusion phase. Tissue samples were collected at specified time points for both ischemia and reperfusion groups. No statistical analyses were conducted on this procedural flow. It is important to note that the 30-minute post-ischemic phase involves passive normothermic saline immersion rather than genuine hemodynamic reperfusion.

Table 3. Composition of the reperfusion solution utilized across all groups

Component	Concentration
Sodium chloride (NaCl)	0.9% (w/v)
Potassium (K^+)	3.0 mmol/L
Calcium (Ca^{2+})	1.2 mmol/L
pH (at 36.5°C)	7.35–7.40
Temperature	36.5°C

Table 4. Comparison of mast cell counts across groups and phases

Phase	**Control (*n* = 8)**	**St. Thomas II (*n* = 8)**	**del Nido (*n* = 8)**	***p* value**
Ischemia	33 (28–39)	33 (27–41)	34 (30–39)	0.95
Reperfusion	29 (22–38)	34 (25–42)	33 (28–38)	0.55
p-value	**0.02**	0.19	0.61	–

Light microscopic ordinal scores, including mast cell counts, leukocytic infiltration, and karyolysis, were analyzed utilizing nonparametric tests. Between-group comparisons were conducted using Kruskal–Wallis tests with Dunn–Bonferroni post-hoc corrections. Data are presented as median (interquartile range, IQR). In the table, statistically significant values are indicated in bold. The *p* value denotes the level of statistical significance, with values less than 0.05 deemed significant.

Table 5. Comparative analysis of leukocytic infiltration scores by group and phase

Phase	**Control (*n* = 8)**	**St. Thomas II (*n* = 8)**	**del Nido (*n* = 8)**	***p* value**
Ischemia	9 (8–10)	10 (10–11)	9 (7–11)	0.10
Reperfusion	10 (9–10)	10 (10–11)	10 (9–10)	0.15
***p* value**	0.11	0.99	0.49	–

Light microscopic ordinal scores, including mast cell counts, leukocytic infiltration, and karyolysis, were analyzed using nonparametric tests. Between-group comparisons were conducted with Kruskal–Wallis tests followed by Dunn–Bonferroni post-hoc corrections. Data are presented as medians with interquartile ranges (IQR). In the table, statistically significant values are highlighted in bold. The p-value reflects the level of statistical significance, with values less than 0.05 deemed significant.

Table 6. Semi-quantitative assessment of karyolytic nuclei in myocardial tissue during ischemia and reperfusion phases

Group	Ischemia phase (median, IQR)	Reperfusion phase (median, IQR)	p value (within group)
Control	2 (1–2)	2 (2–3)	**0.03***
St. Thomas II	2 (1–2)	2 (1–2)	0.12
del Nido	2 (1–2)	2 (1–2)	0.31

Karyolytic nuclear scores during the ischemia and reperfusion phases were evaluated across experimental groups. Karyolysis was graded on a scale of 0 to 3 in H&E-stained sections. A statistically significant increase in karyolytic changes was observed in the control group following reperfusion ($p = 0.03$), whereas the cardioplegia-treated groups exhibited more stable nuclear morphology. Light microscopic ordinal scores, including mast cell counts, leukocyte infiltration, and karyolysis, were analyzed using nonparametric tests. Between-group comparisons were conducted using Kruskal–Wallis tests with Dunn–Bonferroni post-hoc correction. Data are presented as median (interquartile range, IQR).

Table 7. Quantitative ultrastructural parameters of myocardium observed via TEM

Parameter	Control	St. Thomas II	del Nido	*p* value	Effect size (η^2/r)
Flameng score	3.0 (2.5–3.5)	2.0 (1.5–2.5)	0.5 (0–1.0)	**<0.001**	0.78
Crista density (intersections/μm²)	38.2 (30.5–46.1)	55.4 (49.8–60.9)	68.7 (63.1–72.5)	**<0.001**	0.72
Form factor (4π·area/perimeter²)	0.72 (0.68–0.76)	0.79 (0.75–0.82)	0.86 (0.84–0.88)	**0.002**	0.61
Z-line integrity score	2.8 (2.5–3.0)	1.9 (1.5–2.3)	0.7 (0.5–1.2)	**<0.001**	0.65
Basement membrane thickness (nm)	196 (178–215)	154 (140–165)	122 (113–134)	**<0.001**	0.70

Values are reported as median (IQR). Statistical analysis was conducted using the Kruskal–Wallis test, followed by Dunn–Bonferroni correction. A *p* value of less than 0.05 was considered statistically significant. Effect sizes are expressed as η^2 for the Kruskal–Wallis test and as r for pairwise comparisons. Abbreviations: TEM: Transmission electron microscopy; IQR: Interquartile range.

Table 8. Post-hoc Dunn–Bonferroni pairwise comparisons of quantitative TEM parameters

Parameter	Control vs St. Thomas II	Control vs del Nido	St. Thomas II vs del Nido
Flameng score (0–4)	**p = 0.030**, r = 0.51	**p < 0.001**, r = 0.83	**p = 0.010**, r = 0.56
Crista density (intersections/µm²)	**p < 0.001**, r = 0.78	**p < 0.001**, r = 0.86	**p = 0.040**, r = 0.45
Form factor (4π·area/perimeter²)	p = 0.060, r = 0.36	**p = 0.002**, r = 0.62	**p = 0.030**, r = 0.48
Z-line integrity (0–3)	**p = 0.002**, r = 0.64	**p < 0.001**, r = 0.80	**p = 0.010**, r = 0.55
Basement membrane thickness (nm)	**p < 0.001**, r = 0.72	**p < 0.001**, r = 0.84	**p = 0.020**, r = 0.50

The Dunn–Bonferroni correction was implemented, with a two-tailed p-value threshold of < 0.05 deemed statistically significant. Effect sizes (r) were calculated based on pairwise nonparametric rank comparisons.

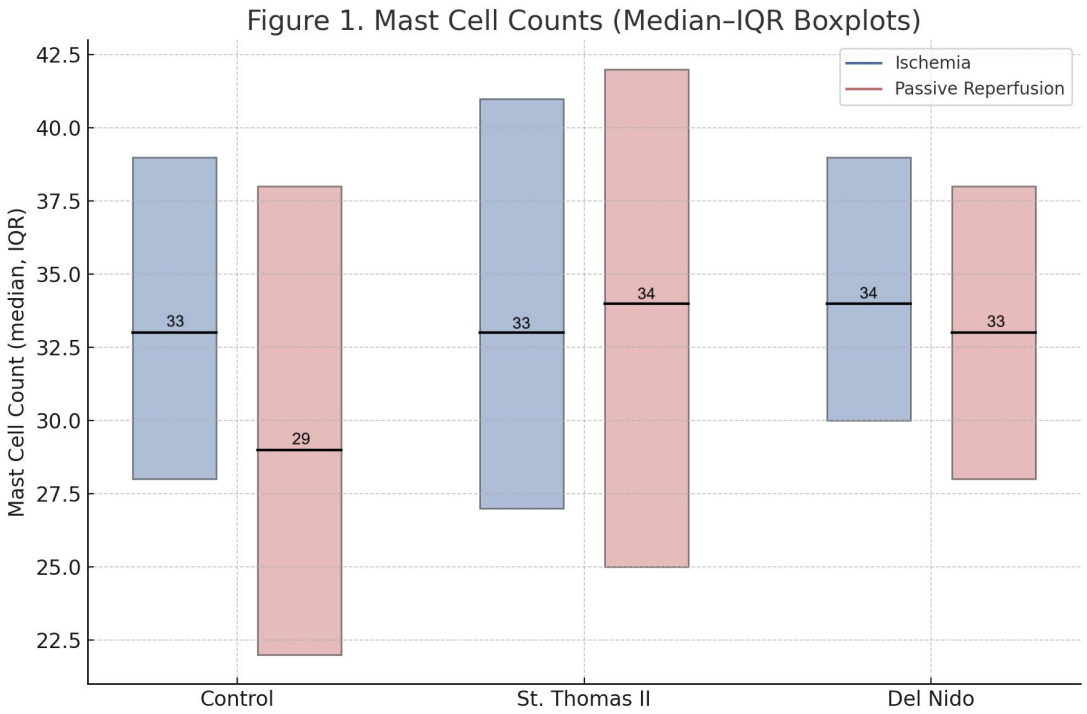

Figure 1. Distribution of mast cell counts during ischemia and reperfusion among the Control, St. Thomas II, and del Nido groups. Data are presented as median and interquartile range, visualized using boxplots. The Control group exhibits a significant decrease in mast cell numbers from ischemia to reperfusion (33 (28–39) → 29 (22–38), $p = 0.02$). In contrast, no significant phase-based changes were observed in either the St. Thomas II or del Nido groups.

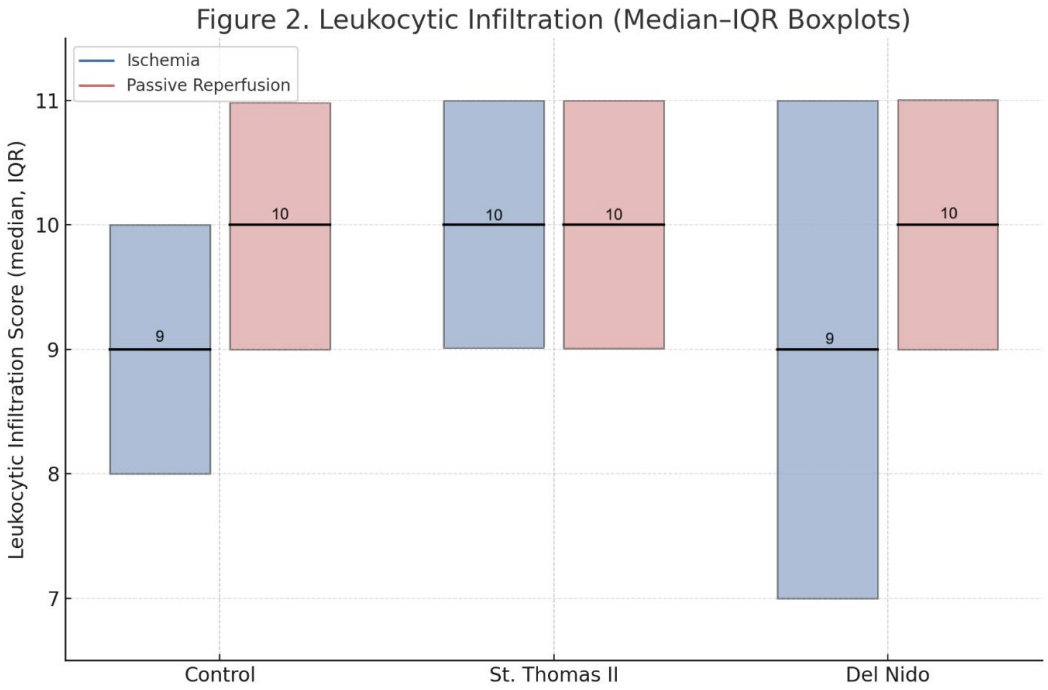

Figure 2. Comparison of leukocytic infiltration scores in ischemia (blue) and reperfusion (red) phases across control, St. Thomas II, and del Nido groups. Data are presented as median and interquartile ranges using boxplot visualization. No statistically significant change was observed within or between groups ($p > 0.05$), indicating that cardioplegia application did not significantly alter leukocyte infiltration.

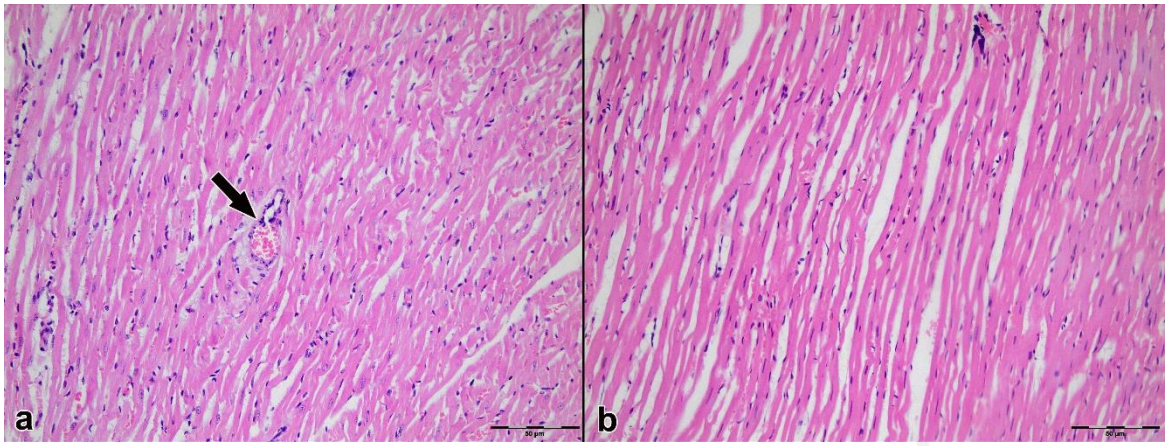

Figure 3. Representative hematoxylin–eosin (H&E)–stained sections of left ventricular myocardium from Group 1 (Control; IR without cardioplegia). (A) Ischemia phase; (B) Reperfusion phase. Cardiomyocytes show preserved overall morphology with regular fiber alignment, homogeneous cytoplasmic staining, and centrally located nuclei; interstitial microvascular profiles remain intact. The arrow indicates an intramyocardial blood vessel. Original magnification ×200.
Abbreviations: H&E: Hematoxylin–eosin; IR: Ischemia–reperfusion.

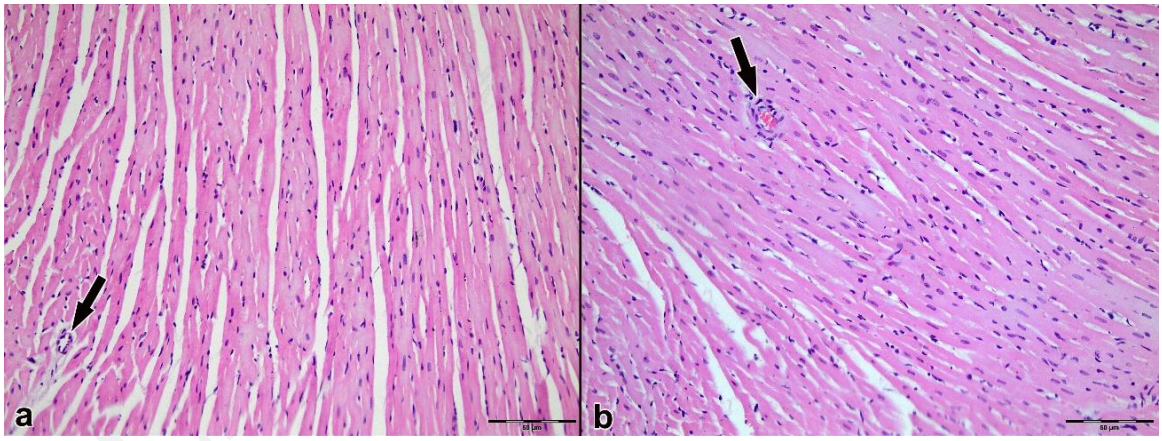

Figure 4. Representative hematoxylin–eosin (H&E)–stained sections of left ventricular myocardium from Group 2 (St. Thomas II cardioplegia). (A) Ischemia phase; (B) Reperfusion phase. Cardiomyocytes demonstrate preserved architecture with regular alignment, homogeneous cytoplasmic staining, and intact, centrally located nuclei; interstitial microvascular profiles remain morphologically intact. Arrows indicate intramyocardial blood vessels. Original magnification ×200.
Abbreviation: H&E: Hematoxylin–eosin.

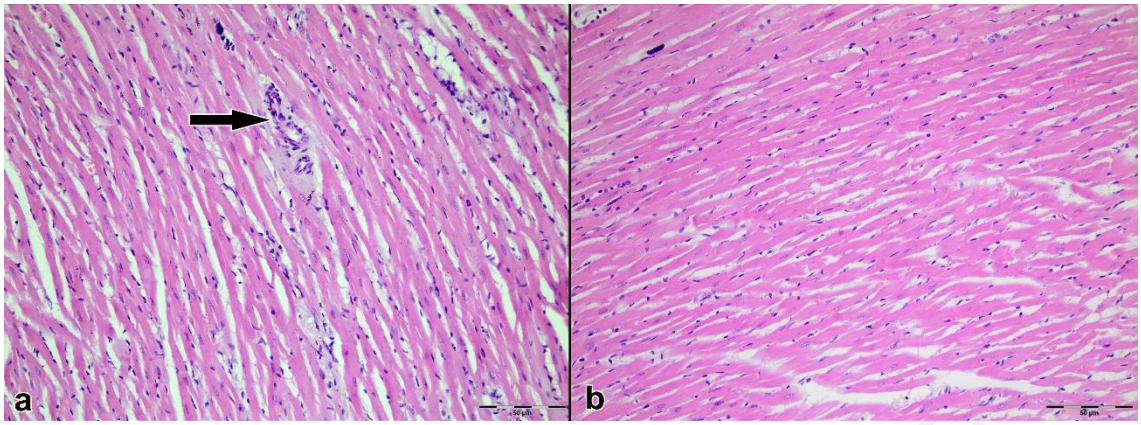

Figure 5. Representative hematoxylin–eosin (H&E)–stained sections of left ventricular myocardium from Group 3 (del Nido cardioplegia). (A) Ischemia phase; (B) Reperfusion phase. Cardiomyocytes show preserved overall morphology with regular fiber alignment, homogeneous cytoplasmic staining, and centrally located nuclei; interstitial microvascular profiles between myocytes remain intact. The arrow indicates an intramyocardial blood vessel. Original magnification ×200. Abbreviation: H&E: Hematoxylin–eosin.

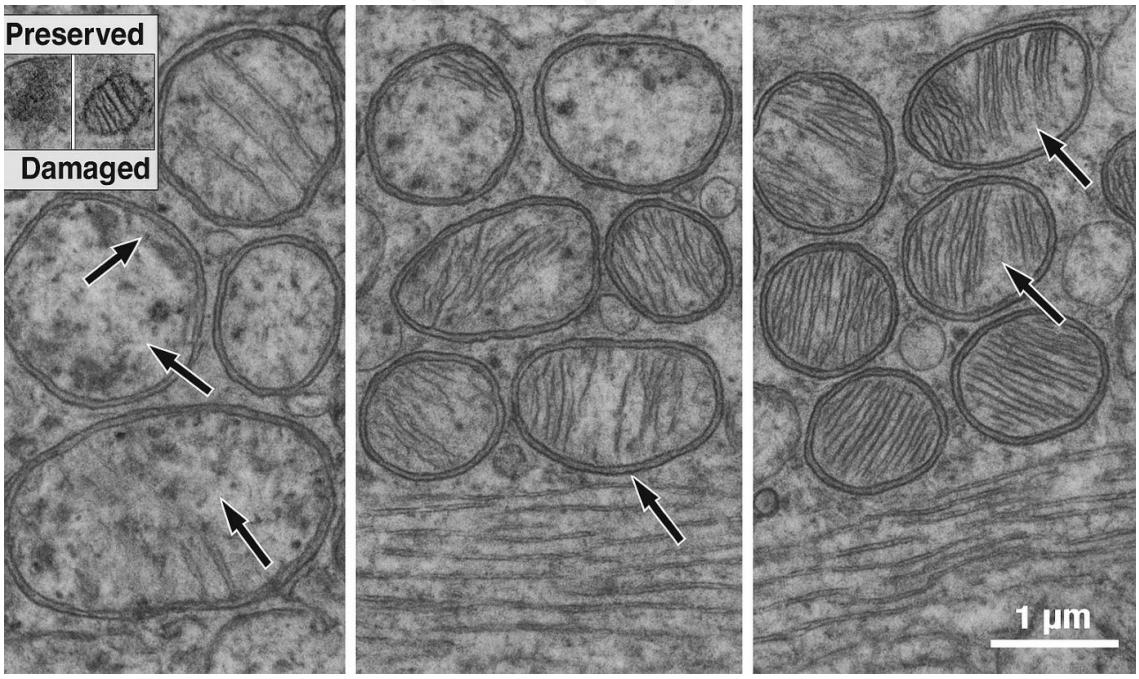

Figure 6. Representative transmission electron micrographs depicting mitochondrial ultrastructure following ischemia-reperfusion injury. The transmission electron microscopy images illustrate mitochondrial morphology across

the experimental groups: left, Control; middle, St. Thomas II; right, del Nido. In the Control panel (left), arrows indicate severely swollen mitochondria, disrupted and fragmented cristae, and areas of matrix rarefaction. In the St. Thomas II panel (middle), arrows highlight partially preserved cristae with moderate mitochondrial swelling. In the del Nido panel (right), arrows denote well-preserved cristae, dense matrices, and intact outer and inner membranes. An inset panel (upper left) provides a direct comparison of preserved versus damaged mitochondria, illustrating intact cristae in the preserved example and crista disruption in the damaged example. All micrographs were captured at approximately ×25,000 magnification, with scale bars representing 1 μm.

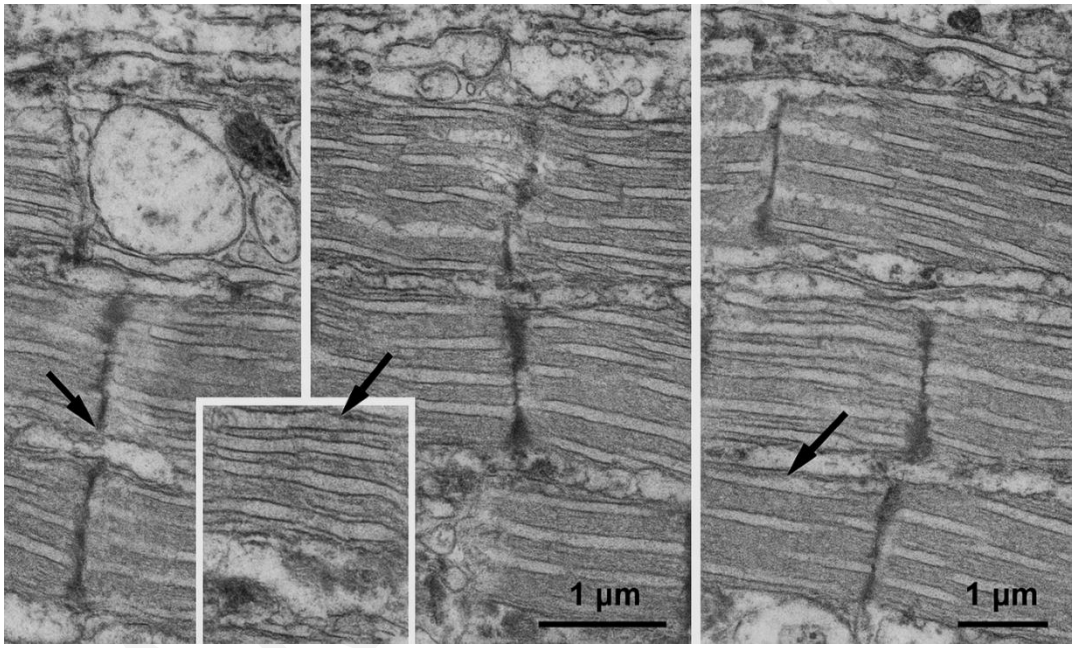

Figure 7. Transmission electron micrographs depicting sarcomeric organization and sarcolemmal morphology following ischemia–reperfusion in rat myocardium. The panels are organized as follows: left, Control; middle, St. Thomas II; right, del Nido. Black arrows indicate areas of sarcolemmal irregularity or blebbing. The Control group exhibits disrupted sarcomeric alignment and focal discontinuities in the sarcolemma. The St. Thomas II group shows partially preserved banding patterns with mild irregularities. In contrast, the del Nido group presents a more uniform sarcomeric periodicity and smoother sarcolemmal contours. The inset panel offers a magnified view of a well-preserved sarcomeric region from the del Nido

sample. All images were captured at approximately ×18,000 magnification, with scale bars representing 1 μm.

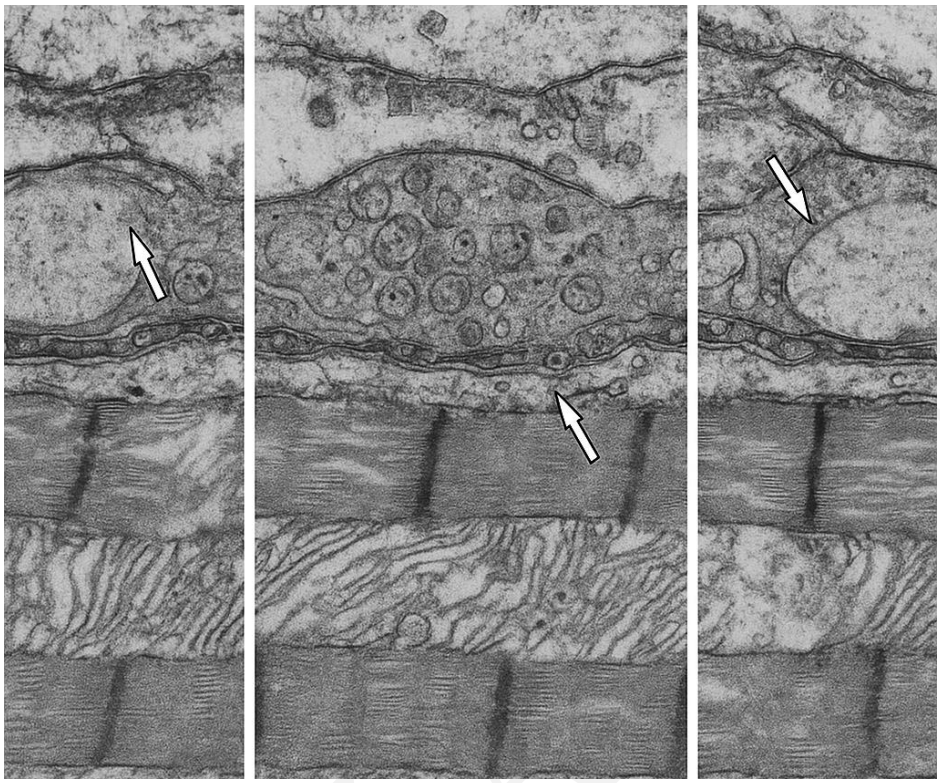

Figure 8. Transmission electron micrographs of myocardial capillary and endothelial ultrastructure following ischemia-reperfusion. Representative TEM images illustrate the ultrastructural changes in myocardial capillaries across the experimental groups: left, Control; middle, St. Thomas II; right, del Nido. In the Control panel (left), arrows indicate severe endothelial swelling, abundant pinocytic vesicles, and markedly thickened basement membranes. In the St. Thomas II panel (middle), arrows highlight localized endothelial protrusions and vesicle clusters, demonstrating partial preservation with focal vesicular dilatation. In the del Nido panel (right), arrows point to thin basement membrane segments and a continuous endothelial lining, reflecting minimal swelling, preserved membrane integrity, and reduced vesiculation. All micrographs were obtained at approximately ×25,000 magnification, with scale bars representing 500 nm. Abbreviation: TEM: Transmission electron microscopy.

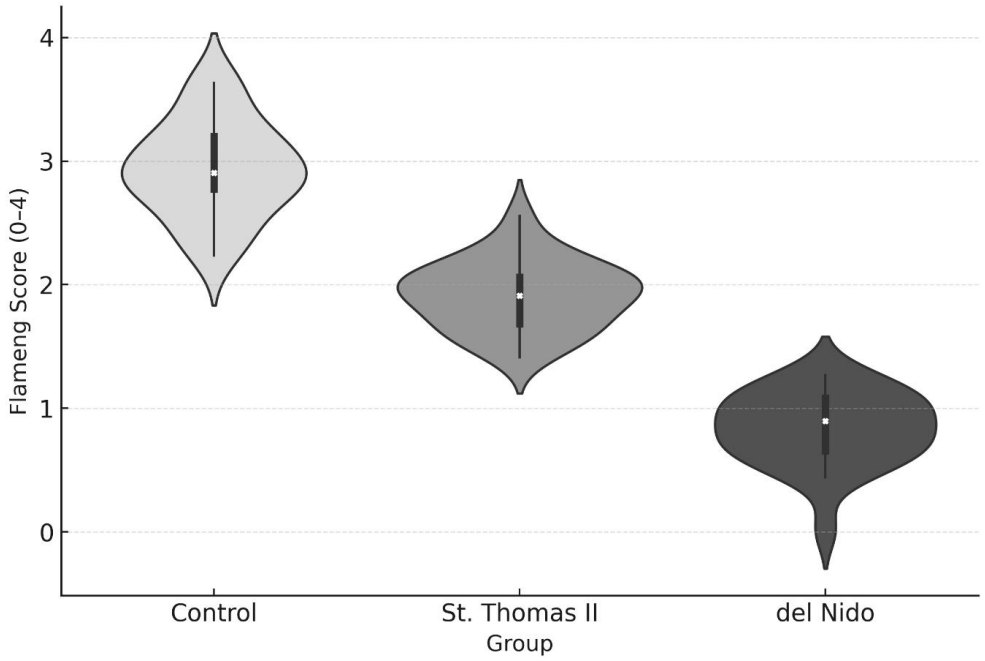

Figure 9. Distribution of flameng scores across experimental groups. Violin and box plots illustrate the distribution of mitochondrial Flameng injury scores among the study groups. The median scores were highest in the Control group, moderate in the St. Thomas II group, and lowest in the del Nido group. The broad distribution observed in the Control group indicates heterogeneous and severe mitochondrial injury, while the del Nido group exhibits a compact clustering around lower scores (0–1), signifying minimal ultrastructural damage. Statistical analysis using the Kruskal–Wallis test followed by Dunn–Bonferroni correction confirmed a significant reduction in Flameng scores in the del Nido group compared to both the Control and St. Thomas II groups ($p < 0.05$).

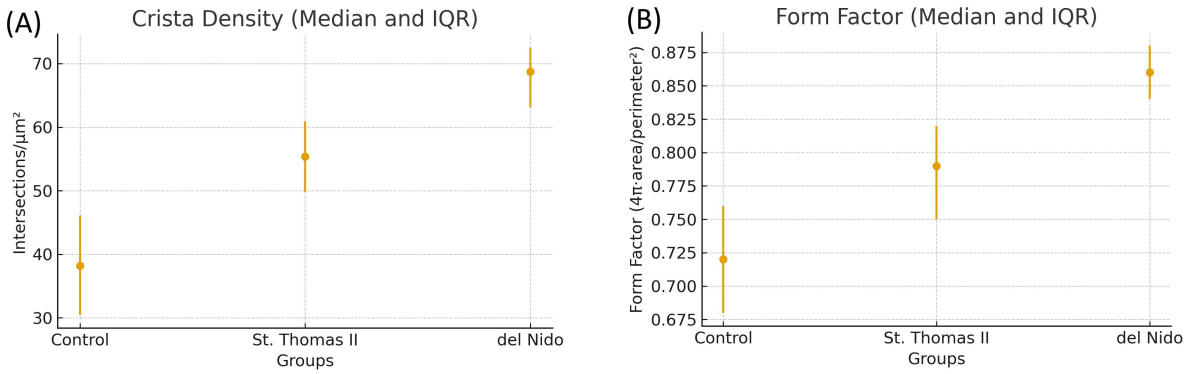

Figure 10. Quantitative mitochondrial ultrastructural metrics across experimental groups (TEM morphometry). (A) Crista density (intersections/µm²) presented as median with interquartile range (IQR). The Control group showed the lowest crista density, St. Thomas II demonstrated intermediate preservation, and the del Nido group exhibited the highest crista density, consistent with superior maintenance of crista organization. **(B)** Mitochondrial form factor ($4\pi \cdot \text{area/perimeter}^2$) presented as median with IQR. Lower values in the Control group indicate greater contour irregularity and outer-membrane distortion; St. Thomas II showed intermediate preservation, whereas del Nido exhibited the most regular mitochondrial morphology. Error bars denote the IQR. Abbreviations: TEM: Transmission electron microscopy; IQR: Interquartile range.

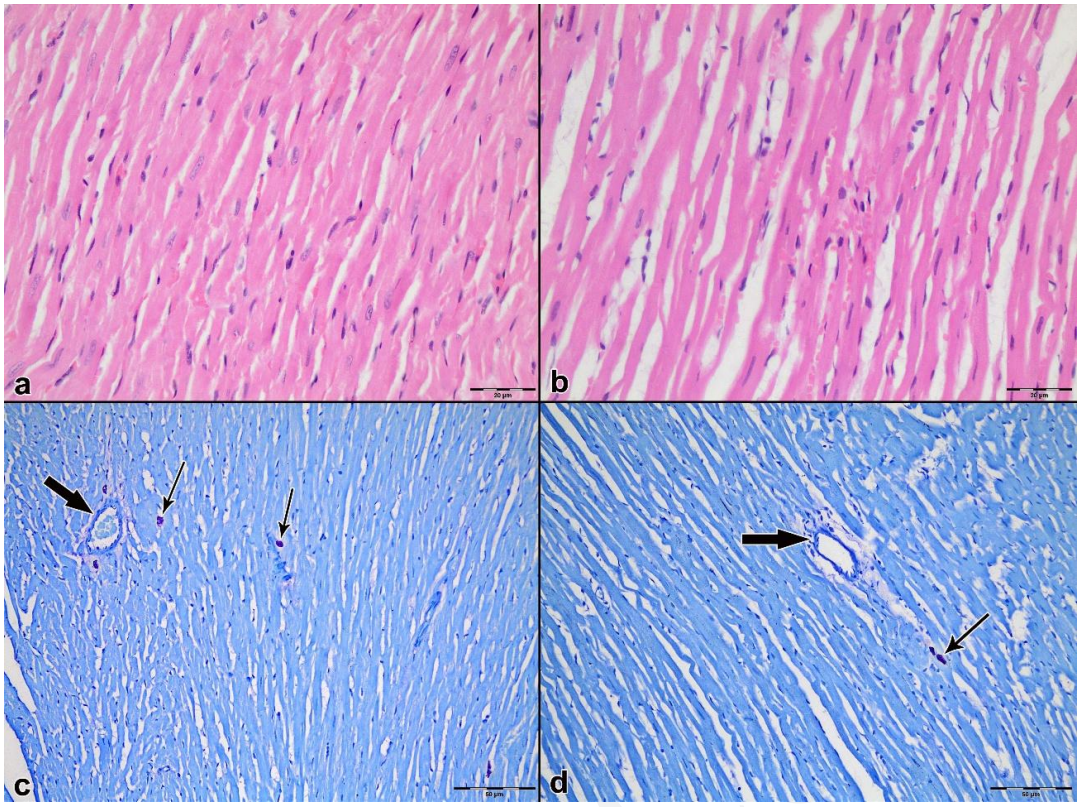

Figure 11. Light microscopic evaluation of myocardium from Group 1 (Control; ischemia–reperfusion without cardioplegia). (A, C) Ischemia phase; (B, D) reperfusion phase. (A, B) Representative hematoxylin–eosin (H&E) sections (original magnification ×400) illustrating overall myocardial architecture. (C, D) Toluidine blue–stained sections (original magnification ×200) highlighting mast cells (thin arrows) in perivascular/interstitial regions; intramyocardial blood vessels are indicated by thick arrows. A visible reduction in mast cell density is observed after reperfusion (D) compared with ischemia (C), consistent with quantitative analysis (33 [28–39] vs 29 [22–38]; $p = 0.02$).

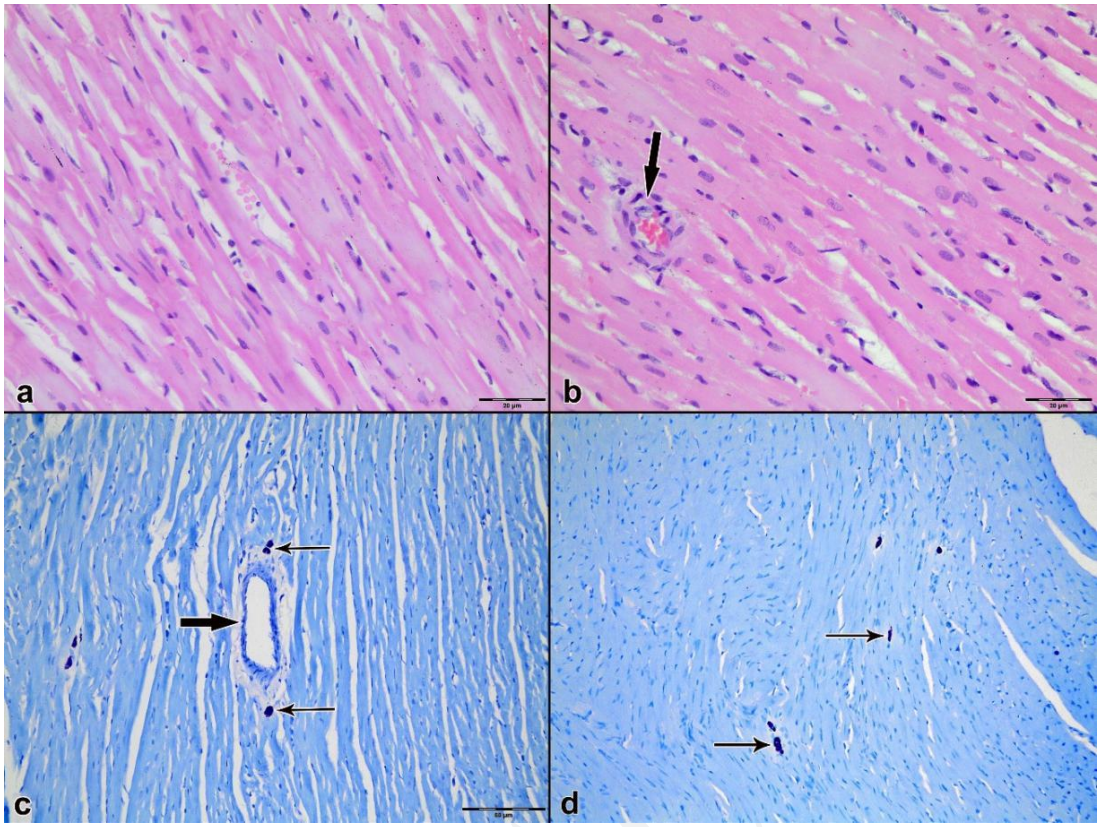

Figure 12. Light microscopic evaluation of myocardium from Group 2 (St. Thomas II cardioplegia). (A, C) Ischemia phase; (B, D) reperfusion phase. (A, B) Representative hematoxylin–eosin (H&E) sections (original magnification ×400) demonstrating preserved myocardial architecture. (C, D) Toluidine blue–stained sections (original magnification ×200) highlighting mast cells (thin arrows) in perivascular/interstitial regions; intramyocardial blood vessels are indicated by thick arrows. Mast cell density appears comparable between ischemia and reperfusion, consistent with quantitative counts (33 [27–41] vs 34 [25–42]; $p = 0.19$).
Abbreviation: H&E: Hematoxylin–eosin.

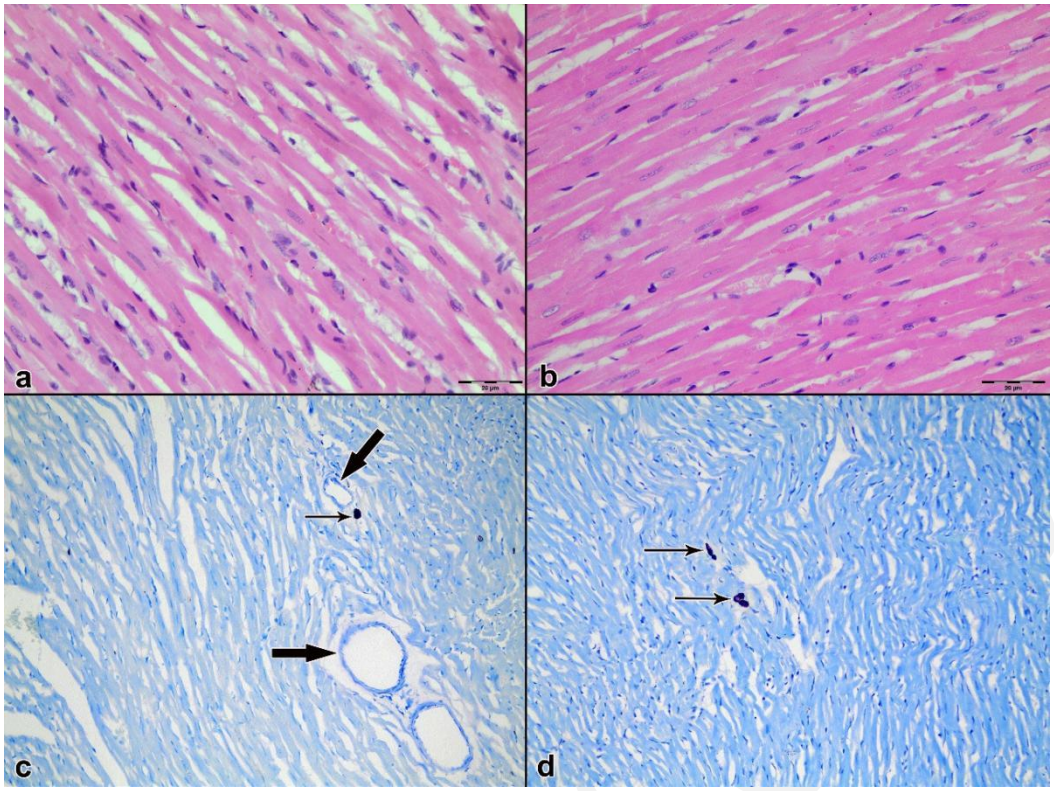

Figure 13. Light microscopic evaluation of myocardium from Group 3 (del Nido cardioplegia). (A, C) Ischemia phase; (B, D) reperfusion phase. (A, B) Representative hematoxylin–eosin (H&E) sections (original magnification ×400) showing preserved myocardial architecture. (C, D) Toluidine blue–stained sections (original magnification ×200) highlighting mast cells (thin arrows) in perivascular/interstitial regions; intramyocardial blood vessels are indicated by thick arrows. Mast cell density appears stable between ischemia and reperfusion, consistent with quantitative counts (34 [30–39] vs 33 [28–38]; $p = 0.61$). Abbreviation: H&E: Hematoxylin–eosin.

SUPPLEMENTAL DATA

Key points

a. What is known about the topic?

- Myocardial ischemia–reperfusion injury is a major contributor to perioperative morbidity in cardiac surgery.
- Cardioplegia solutions such as St. Thomas II and del Nido are widely used to minimize ischemic damage, yet comparative histological and ultrastructural evidence in experimental settings remains limited.
- While del Nido cardioplegia offers pharmacological advantages due to its lidocaine and mannitol components, St. Thomas II has long been considered a reliable standard for myocardial protection.

b. What does this study add?

- This study provides the first integrated light microscopic and transmission electron microscopic comparison of St. Thomas II and del Nido cardioplegia in a controlled rat ischemia–reperfusion model.
- Both cardioplegia solutions preserved myocardial histological architecture, stabilized mast cell counts, and reduced inflammatory cell infiltration compared with untreated controls.
- Transmission electron microscopy, the predefined primary endpoint of the study, demonstrated statistically significant ultrastructural superiority of del Nido cardioplegia over St. Thomas II—including lower Flameng scores, higher crista density, improved Z-line continuity, and thinner basement membranes.
- These findings indicate that although light microscopic parameters appear comparable between the two solutions, del Nido provides more robust mitochondrial and microvascular preservation at the ultrastructural level.